Title

Differential methylation, epigenetic clocks, and island-mainland divergence in an insectivorous small mammal

Authors

Marie-Laurence Cossette[1*], Donald T. Stewart[2], Amin Haghani[3], Joseph A. Zoller[4], Aaron B.A. Shafer[1,5*], Steve Horvath[3,4]

Affiliations:

[1]Dept. of Environmental Life Sciences Graduate Program, Trent University, Peterborough, ON, Canada

[2]Dept. of Biology, Acadia University, Wolfville, NS, Canada

[3]Dept. of Human Genetics, David Geffen School of Medicine, University of California Los Angeles, Los Angeles, CA, USA

[4]Dept. of Biostatistics, Fielding School of Public Health, University of California Los Angeles, Los Angeles, CA, USA

[5]Dept. of Forensic Science, Trent University, Peterborough, ON, Canada

[*]Corresponding authors: mcossette@trentu.ca; aaronshafer@trentu.ca

Abstract

Geographically isolated populations, including island-mainland populations, tend to exhibit phenotypic variation in many species. The so-called island syndrome occurs when different environmental pressures lead to insular divergence from mainland populations. This phenomenon can be seen in an island population of Nova Scotia masked shrews (*Sorex cinereus*), which have developed a specialized feeding habit and digestive enzyme compared to their mainland counterparts. Epigenetic modifications, such as DNA methylation (DNAm), can impact phenotypes by altering gene expression without changing the DNA sequence. Here, we used a *de novo* masked shrew genome assembly and epigenome-wide assay to investigate morphological and DNA methylation patterns between island and mainland populations. Island shrews were morphologically and epigenetically different than their mainland counterparts, exhibiting a smaller body size; remarkably, the gene ontology analyses mirrored these phenotypes including genes for the digestive enzyme phenotypes. Moreover, island shrews appeared to age faster than their mainland counterparts. This study provides an example counter to the prevailing island syndrome morphological patterns, along with novel epigenomic insight into the drivers of island-mainland divergence in mammals.

Keywords

epigenetic clock, DNA methylation, masked shrew, genome assembly, island divergence, island rule

Introduction

Insular populations tend to exhibit distinctive traits compared to their continental counterparts (Adler & Levins, 1994; Foster, 1964; Goltsman et al., 2005; Meröndun et al., 2019; Novosolov et al., 2013; van Valen, 1973). This phenomenon is known as the island syndrome and refers to ecological, physiological, behavioural, and morphological differences between island and mainland populations (Baeckens & van Damme, 2020). Different pressures such as altered predation, competition, environment, and geographic isolation are thought to lead to phenotypic differences between mainland and insular populations (Baeckens & van Damme, 2020; Benítez-López et al., 2021; Lomolino et al., 2013). Body size varies in the context of island-mainland comparisons for many species, where some insular populations exhibit dwarfism or gigantism (Foster, 1964; Herridge & Lister, 2012; Thomson et al., 2018). The 'island rule' hypothesizes that smaller animals tend to increase in size, while larger ones tend to decrease in size on islands (Lomolino, 1985; Lomolino et al., 2013; van Valen, 1973). This pattern has been observed in mammoths (*Palaeoloxodon falconeri*) (Herridge & Lister, 2012) and deer mice (*Peromyscus maniculatus*) (Miller et al., 2021), but counter and ambiguous examples exist (Juette et al., 2020; Lokatis & Jeschke, 2018; Meiri et al., 2006, 2008).

Relatively little is known about the specific mechanisms causing phenotypic changes in each of these cases, whether it be genetic drift, natural selection, or plasticity (Baeckens & van Damme, 2020; Benítez-López et al., 2021). Miller et al. (2021) found heritable variations for deer mice for both mass and length associated with outlier loci between island-mainland populations, suggested that natural selection underlies such phenotypic divergence. Island-mainland populations, however, do not always exhibit clear signal of nuclear genetic divergence with divergent phenotypes (e.g., Meröndun et al., 2019; Vernaz, Malinsky, et al., 2021). In contrast,

69 different epigenetic signatures – defined as chemical modifications that regulate gene expression
70 (Al Aboud et al., 2021) – have been associated with substantial levels of divergence between
71 species and populations with different phenotypes (Meröndun et al., 2019; Vernaz, Malinsky, et
72 al., 2021) and unlike DNA, epigentic structures can respond quickly to environmental pressures
73 (Anastasiadi et al., 2021).

74 Epigenetic changes can be heritable and have been associated with early stages of
75 speciation (Quadrana & Colot, 2016; Vernaz, Hudson, et al., 2021; Vernaz, Malinsky, et al., 2021;
76 Vogt, 2017). Epigenetic modifications can regulate gene expression through chemical or structural
77 modifications without directly changing the DNA sequence (Razin & Riggs, 1980). DNA
78 methylation (DNAm) involves the transfer of a methyl group to a cytosine base, mostly occurring
79 on CpG sites (Moore et al., 2013). Some regions of the genome, called CpG islands (CGI), contain
80 a high frequency of CpG dinucleotides and these are known to overlap most promoter regions in
81 mammals (Gardiner-Garden & Frommer, 1987; P. A. Jones, 1999). These sites appear to be
82 evolutionarily important as they are highly conserved across vertebrates (Illingworth & Bird, 2009;
83 Ioshikhes & Zhang, 2000; McLain & Faulk, 2018). Mechanisms like DNAm allow individuals to
84 respond quickly to environmental changes. Over time, differential methylation can lead to
85 permanent heritable (cis) nuclear changes referred to as genetic assimilation (Anastasiadi et al.,
86 2021). This can happen when environmental conditions persist through generations favouring a
87 specific phenotype, and overtime resulting in selection for a permanent genetic basis (e.g., point
88 mutations) for the phenotype previously produced from the plastic epigenetically-influenced
89 phenotype (Anastasiadi et al., 2021).

90 Differential methylation patterns in wild and captive populations have been associated with
91 phenotypic traits such as body size in sheep (*Ovis ammon*) (Cao et al., 2015) and lynx (*Lynx*

92 *canadensis*) (Meröndun et al., 2019), pigmentation levels in rabbits (*Oryctolagus cuniculus*) (Chen
93 et al., 2021) and breeding success in barn swallows (*Hirundo rustica*) (Saino et al., 2017). In
94 addition, the rate of DNAm, particularly hypermethylation, on specific CpG sites changes
95 throughout an individual's lifetime, making it possible to age individuals based on their
96 methylation levels (Horvath, 2013; Lu et al., 2021; Prado et al., 2021; Wilkinson et al., 2021).
97 These epigenetic *clocks*, while they can predict chronological age (Jasinska et al., 2021; Lu et al.,
98 2021; Prado et al., 2021; Raj et al., 2021; Schachtschneider et al., 2021), have also been shown to
99 be elevated in inbred individuals, suggesting that inbreeding can lead to aging at a faster rate
100 compared to non-inbred individuals (Larison et al., 2021). Likewise, metabolic syndrome in
101 humans (i.e., hypertension, obesity) also results in increased epigenetic aging (Lee & Park, 2020;
102 Nannini et al., 2019). It stands to reason that the differential selection pressures underlying island-
103 mainland patterns might also alter the DNAm aging rate, especially when body size differs
104 markedly.

105 The shrew family (Soricidae) appeared about 30 to 40 million years ago (Churchfield,
106 1990). Hundreds of extant shrew species are now found on most continents (Churchfield, 1990;
107 George, 1986, 1988). Some shrews have evolved unique traits such as echolocation (Chai et al.,
108 2020; Forsman & Malmquist, 1988; Tomasi, 1979), venomous saliva (Kita et al., 2004) and the
109 ability to dive underwater (Catania et al., 2008; Mendes-Soares & Rychlik, 2009). Shrews have
110 the fastest mass-specific metabolic rate of all mammals (Ochocińska & Taylor, 2005) and are one
111 of the smallest and shortest-lived mammals making them important to study from an aging
112 perspective (Lu et al., 2021). Shrews of the genus *Sorex* show differing trends in body size
113 variation across their range; populations of some species at higher latitudes have smaller body
114 sizes, which is counter to the predictions of Bergmann's rule (Ochocinska & Taylor, 2003; Yom-

115 Tov & Yom-Tov, 2005), whereas populations of some other species are larger at more northerly
116 latitudes (Huggins & Kennedy, 2018). *Sorex* shrews exhibit highly plastic phenotypes; the
117 Eurasian common shrew (*Sorex araneus*), for example, manifests seasonal and reversible changes
118 in skull morphology, body mass and organ size (Lázaro et al., 2017; Schaeffer et al., 2020; Taylor
119 et al., 2013). Whether plastic or genetic in nature, these phenotypic variations throughout winter
120 and latitude are generally explained as a response to limited resource availability (Lázaro et al.,
121 2017; Ochocińska & Taylor, 2003; Ochocinska & Taylor, 2003; Schaeffer et al., 2020; Taylor et
122 al., 2013; Yom-Tov & Yom-Tov, 2005).

123 Masked or Cinereus shrews (*Sorex cinereus*) are the most abundant shrew in North
124 America (Nagorsen, 1996). The range of this species spans much of the northern United States and
125 most of Canada (Nagorsen, 1996). Although they tend to eat a variety of invertebrates, the masked
126 shrew has a varied diet across its range (Bellocq et al., 1994; Churchfield, 1990; Whitaker John O.
127 Jr. & French, 1984). Of note, an isolated population of island dwelling masked shrews is known
128 to have developed a specialized feeding habit in response to their different environment and diet
129 (Stewart et al., 1989); masked shrews on Bon Portage Island (BPI) off the southern coast of Nova
130 Scotia are the only population of *Sorex* shrews known to mainly feed on sand fleas (*Platorchestia*
131 *platensis*) (MacPherson & Stewart, 2003; Stewart et al., 1989). *Platorchestia platensis* is a type of
132 amphipod typically not consumed by insectivores, although Churchfield (1990) notes that the
133 population of the lesser white-toothed shrew (*Crocidura suaveolens)* on St. Martin's, Isles of
134 Scilly, in the United Kingdom, also feed on amphidods. In the case of *S. cinereus*, it is hypothesized
135 that due to the importance of sand fleas on BPI, the shrew's digestive enzyme, Peptidase A, has
136 undergone an adaptive response (MacPherson & Stewart, 2003), though empirical support is
137 limited (MacPherson & Stewart, 2003; McAlpine, 2009). Here, using a *de novo* assembled and

138 annotated genome, we quantified differential methylation patterns between populations of masked
139 shrews to test whether insular masked shrews have epigenetically diverged from mainland
140 populations. We hypothesized that island shrews will exhibit different phenotypes than mainland
141 shrews based on the island syndrome and that divergent methylation patterns will underly this. We
142 further predicted that BPI shrews will have differential methylation patterns associated with
143 digestive enzymes compared to mainland shrews.
144

145 **Materials and methods**

146 **Sampling, sexing, and aging shrews**

147 Masked shrew samples were collected from five locations: Peterborough County (44°53′N,
148 78°05′W) in Ontario, Canada, and Sandy Cove (44°48′N, 66°08′W), North Mountain (45°13′N,
149 64°22′W), Long Island (44°19′N, 66°16′W) and Bon Portage Island (BPI) (43°28′N, 65°45′W) in
150 Nova Scotia, Canada. All shrews were trapped between mid-July and late August to limit seasonal
151 morphological differences, such as skull and body size (Lázaro et al., 2019, 2021). DNA was
152 extracted from liver, tail, and fetal tissue using the DNeasy Blood & Tissue Kit from QIAGEN.
153 Shrews were left in dermestid beetle tanks for a week to remove all remaining tissue from the
154 skulls. A Leica EZ4 microscope was used to assess age class for each shrew based on teeth wear
155 according to the method of Pruitt (Pruitt, 1954; Rudd, 1955). Age in months was estimated based
156 on the trapping date, the age class, and the known reproductive season of masked shrews assuming
157 a maximum lifespan of ~17 months (Churchfield, 1990). Age class designations were confirmed
158 based on morphological features (Pruitt, 1954; Rudd, 1955). Shrews were sexed by gel
159 electrophoresis of PCR amplicons of the Y chromosome-linked SRY gene (Cervantes et al., 2013;

160 Matsubara et al., 2001) using custom primers (Table S1); sex assignments were subsequently
161 validated with the methylation assay (Wang et al., 2021).
162
163 **Genome assembly and annotation**
164 A single masked shrew from Peterborough County, Ontario had DNA and RNA extracted from
165 the heart and liver immediately after euthanasia. We used the MagAttract HMW DNA Kit from
166 QIAGEN and the Monarch Total RNA Miniprep Kit from New England BioLabs respectively and
167 sent the extracts to The Centre for Applied Genomics, Toronto, Ontario, Canada, for sequencing.
168 Short-read (SR) libraries were generated using Truseq PCR-free preparation and sequenced on two
169 lanes on an Illumina HiSeq X platform with 150 bp paired-end reads. Linked reads (LR) were
170 prepared using the 10X genome library after selecting fragments >20Kb using BluePippin. The
171 linked reads were sequenced on one Illumina HiSeq X Lane. Twenty-five million RNA reads were
172 sequenced on a HiSeq2500 with 126bp paired-end reads.
173 We used BBMap v. 35.8 (Bushnell, n.d.) to remove adapters and trim low-quality data
174 from the fastq files. Contaminant screening was performed using Kraken2 v. 2.0.9-beta (Wood &
175 Salzberg, 2014) and all unclassified sequences were kept. Kmergenie v. 1.7048 (Chikhi &
176 Medvedev, 2014) was used to find the kmer size for downstream analysis. The genome was
177 assembled using a tiered approach: i) using only the SR data and Meraculous v.2.2.4 (Chapman et
178 al., 2011); ii) with only the LR data using Supernova v.2.1.1 (Weisenfeld et al., 2018) using the --
179 maxreads filter set to "all". The pseudohap2 style was selected for the assembly output. Following
180 the assembly, both SR and LR assembly versions were merged via quickmerge v.0.3 (Chakraborty
181 et al., 2016) with the LR as the backbone. Scaff10x v.5.0 (Ning et al., n.d.) was used to further
182 polish the *S. cinereus* genome. Genome completeness was assessed using Benchmarking Universal

183 Single-copy Orthologs (BUSCO) v.3.0.2 (Simão et al., 2015) by comparing the hybrid genome to
184 highly conserved genes in mammals based on the *mammalia_odb9* dataset. The mitochondrial
185 genome was assembled using MitoZ v.2.4-alpha (Meng et al., 2019). Genome annotation was
186 conducted via GenSAS v.6.0 (Humann et al., 2019) using the assembled genome and RNAseq
187 data. Here, repeat regions of the genome were identified using RepeatModeler v.1.0.1.1 (Smit &
188 Hubley, n.d.-b) and RepeatMasker v.4.0.7 (Smit & Hubley, n.d.-a). Masked shrew liver and heart
189 RNA reads were mapped to the genome using HISAT2 v.2.1.0 (Kim et al., 2019). The resulting
190 BAM file was used by BRAKER v.2.1.1 (Hoff et al., 2019) and EVidenceModeler v1.1.1 (Haas
191 et al., 2008) to predict features in the genome. Functional annotation to find common protein
192 sequences between the masked shrew and the common shrew, *Sorex araneus* (GenBank assembly
193 accession: GCA_000181275.2), and other vertebrate mammals was done using BLAST v.2.11.0
194 (Altschup et al., 1990), SwissProt v.2.11.0 (Bairoch & Apweiler, 1998) and InterProScan v.5.44-
195 79.0 (P. Jones et al., 2014) databases.
196
197 **Epigenetic clocks**
198 DNA methylation profiles for each sample were assayed on the HorvathMammalMethylChip40,
199 a novel Infinium array (Arneson et al., 2022) that screens over 37,000 CpGs. The SeSaMe
200 normalization method was used to define beta values for each probe (Zhou et al., 2018). Only
201 probes that aligned to the masked shrew genome (bwa-mem) were retained for downstream
202 analysis. Elastic net regressions were applied to the DNAm data and the chronological age
203 estimates to construct the masked shrew epigenetic clock. Three different models were used as per
204 Lu et al. (2021); 1) no transformation to the chronological age, 2) log-transformed chronological
205 age (log(x+1)), and 3) square root transformed chronological age (sqrt(x+1)) with offsets of 1 year

206 to avoid negative values for our fetal samples. To assess the accuracy of our models we used a
207 leave-one-out (LOO) cross-validation with estimate outputs for the correlation as well as the
208 median absolute error between predicted DNAm age and actual chronological age (years).
209

210 **Statistical analyses and functional gene enrichment**

211 We ran a series of models in R v.1.3.959 (R Core Team, 2021). Using linear models, we separately
212 regressed body size, weight, and skull length against location, age and sex (i.e., phenotype ~
213 location + age + sex). Here, location was a categorical variable of island or mainland (see Table
214 1). Additionally, we extracted the residuals from the epigenetic clock for each sample and ran a
215 Welch Two Sample T-test using location and sex as groupings. Positive residuals were indicative
216 of an epigenetically older individual than the linear model would predict.

217 Epigenome-wide association studies (EWAS) were conducted using the limma package
218 v.3.44 (Ritchie et al., 2015); note we removed the fetal samples from this analysis. Using the β
219 values of aligned probes, we ran the following model: DNAm ~ location + sex + age + tissue
220 including animal ID as a random effect. This model was run two times; once with BPI and Long
221 Island grouped together as 'Island' in the model with all other locations assigned as 'Mainland',
222 and once with BPI versus all other populations. The latter grouping was meant to isolate possible
223 unique dietary adaptations of BPI shrews. A p value $< 2e\text{-}6$ was set according to the Bonferroni-
224 corrected threshold as the cutoff for significance to be conservative (Johnson et al., 2010).
225 Enriched pathways associated with the significant CpGs for the EWAS models were identified
226 with rGREAT v.1.20 (McLean et al., 2010) using the human Hg19 genome annotation to allow
227 for comparisons (Jasinska et al., 2021; Prado et al., 2021; Schachtschneider et al., 2021). We
228 accounted for bias resulting from the design of the mammalian array by using 14,290 CpGs that

229 mapped to our shrew annotations as background. Following Schachtschneider et al. (2021), from
230 these probes the top 500 hypermethylated and top 500 hypomethylated sites were used for the
231 enrichment analysis.
232
233 **Results**
234 **Genome assembly and annotations**
235 The SR and LR assembly statisitcs are provided in Table S2; the final hybrid genome was 2.66 Gb
236 with an N50 of 1.99 Mb and L50 of 291. The GC content was 42.88% with over 86% of the
237 genome being in scaffolds over 50 Kb and the largest scaffold being around 22 million base pairs.
238 Close to 95% of BUSCOs were identified in this assembly (Table S2): 3504 of 4101 were complete
239 single-copies, 74 were complete duplicates and 301 were fragmented. Repeats represented 38.60%
240 of the genome (Table S3) with long interspersed nuclear elements (LINEs) and unclassified repeats
241 representing 20.17% and 15.39% of the genome respectively. The functional annotation pipeline
242 identified 20,067 protein coding genes (Table S2). The raw sequence data have been deposited in
243 the Short Read Archive (SRA) under accession number PRJNA826195. The assembly has been
244 deposited at DDBJ/ENA/GenBank (accession no. pending).
245
246 **Epigenetic clocks**
247 The methylation data consisted of 48 high quality tail, liver, and fetal tissue DNA samples from
248 37 different individuals. The average age of our samples was seven months; the youngest shrews
249 being fetuses and the oldest one being an estimated 16 months (Table 1, Table S4). Out of the
250 37,000 probes, 29,609 were aligned to our masked shrew genome. We constructed and cross-
251 validated epigenetic clocks for different masked shrew tissue types, which included liver, tail,

252 fetus, and pan-tissue clock. The final clocks were based on the methylation profiles of 26 CpGs
253 and included the age correlation between the estimate DNAm age and the chronological age and
254 the median absolute error (MAE). Our clocks were highly accurate with correlation values of 0.91
255 and an average MAE of 0.13 years for the pan-tissue clock, representing approximately a 7-week
256 difference between the estimated DNAm age and the teeth-based chronological age. The liver
257 DNAm clock had the lowest MAE of 0.07 years (~3 weeks), followed by the pan-tissue and tail
258 clocks with MAE around 0.1 (~5 weeks) (Figure 1).
259
260 **Island-mainland differences**
261 Mass, body length and skull length differed between the mainland and island samples (Figure 2).
262 Our models including age, sex, and island-mainland covariates explained a high percentage of
263 variance: skull length (R^2 = 0.81), weight (R^2 = 0.55) and body length (R^2 = 0.47; Table 2). In all
264 models, location was the most important variable correlated to the change in body size and weight
265 (*p* value < 0.01; Table 2). All size metrics were negatively correlated to being on an island (Figure
266 2). Age was positively correlated to body size whereas sex did not have an effect (Table 2).
267 Epigenetic clocks were slightly elevated on islands (t = -1.95, df = 39.73, *p* value = 0.06); here the
268 residual variation was higher on the island (mean of 0.01) compared to the mainland (mean of -
269 0.02). There was no difference in residuals among the sexes (t = -0.97, df = 40.2, *p* value = 0.34)
270 or age groups (yearlings vs older) (t = -0.21, df = 11.79, *p* value = 0.84).
271
272 **EWAS Island effects**
273 A total of 1067 CpG sites (482 hypermethylated and 585 hypomethylated) were identified (*p* value
274 < 2e-6) between our island and mainland populations (Figure 3A). The most divergent CpG was

275 near the *EWS* exon (*p* value = 3.35e-21) a gene that encodes a multifunctional protein involved in
276 various cellular processes such as gene expression, cell signaling, and RNA processing and
277 transport. Top CpGs were proximal to genes associated to developmental and adipose-related
278 processes: (*MEST* exon (*p* value = 3.34e-14), *SIM1* intergene (*p* value = 3.79e-13), *PHIP* intergene
279 (*p* value = 1.03e-12)) and metabolism: *ZBTB7C* promotor (*p* value = 8.45e-14) and *ATPA* exon (*p*
280 value = 6.37e-16) (Table 3, Figure 3A, 3B). The top hypermethylated CpGs were near genes
281 associated with three different fibroblast growth factor receptors pathways (*p* value < 5e-16)
282 (Figure 3C). Other significantly enriched pathways included synaptic and adipose-related
283 processes (Figure 3C).

284 Isolating BPI from the other populations identified 485 significant CpGs (*p* value < 2e-6),
285 308 were hypomethylated and 177 were hypermethylated (Figure 4A). The top significant
286 hypomethylated CpG in BPI samples was near the *SMO* exon (*p* value = 1.42e-30; Table 3, Figure
287 4A, 4B). Top CpGs were most often hypomethylated in BPI island samples (Table 3, Figure 4A,
288 4B). Pathway analysis highlighted that differentially methylated sites in BPI shrews compared to
289 other populations seem to affect digestive and intestinal phenotypes and functions (Figure 4C).
290 Additionally, other phenotypes related to skull morphology, more specifically the mandible, teeth,
291 and ear canal showed pathway enrichment in BPI shrews (Fig 4C).

292

293 **Discussion**

294 The island syndrome describes the distinctive morphological differences between island-mainland
295 populations due to different ecological and environmental pressures (Baeckens & van Damme,
296 2020). We tested whether phenotypic divergence occurred via epigenetic modifications,
297 specifically DNA methylation, which alter gene expression without changing the DNA sequence

298 (Razin & Riggs, 1980). Over 29,000 probes aligned to our genome, consistent with other
299 mammalian studies (Larison et al., 2021; Pinho et al., 2021; Schachtschneider et al., 2021; Sugrue
300 et al., 2021), and a robust epigenetic clock was generated (Figure 1). The differential methylation
301 between island-mainland populations showed a remarkable overlap between enriched pathways
302 and measured phenotypic differences. While some association assessments suffer from false
303 positives and story-telling (Pavlidis et al., 2012), there was an unambiguous connection to the
304 measured phenotypes (Figure 2), dietary differencs (MacPherson & Stewart, 2003; McAlpine,
305 2009; Stewart et al., 1989), and the observed enriched pathways (Figure 3, 4). Thus, the clear
306 morphological and dietary island-mainland differences appear to be, in part, under epigenetic
307 influence.
308
309 **Phenotypic divergence**
310 DNA methylation regulates gene expression thereby contributing to phenotypic plasticity (al
311 Aboud et al., 2021; Kooke et al., 2015; Razin & Riggs, 1980), which can lead to phenotypic
312 variation among individuals subject to different environmental conditions (Anastasiadi et al., 2021;
313 Kooke et al., 2015; Meröndun et al., 2019). Here, insular masked shrews exhibited different
314 phenotypes than their mainland counterparts; morphologically, this presented as decreased body
315 length, mass, and skull length on islands. Body size is a polygenic trait (Posbergh & Huson, 2021)
316 with many underlying mechanisms, often making it difficult to clearly understand the role of each
317 gene or pathway involved (e.g., Anderson et al., 2022). DNA methylation has been suggested as a
318 universal mechanism that regulates body mass and morphological development in animals (Cao et
319 al., 2015; Haghani et al., 2021), and appears to help regulate intra-species differences in island-
320 mainland settings.

321 Differential methylation patterns between island and mainland shrew populations included
322 fibroblast growth factors (FGF), which are crucial for animal body development (Oulion et al.,
323 2012), and adipose-related genes and processes. Haghani *et al.* (2021) also found that across
324 mammals, species weight was correlated to development and adipose-related pathways. In masked
325 shrews, CpGs proximal to the homolog to mesoderm-specific transcript protein (*MEST*) and
326 single-minded homolog 1 (*SIM1*) genes were hypo and hypermethylated respectively in island
327 shrews. *MEST* is known to be correlated to adipocytes in humans (Karbiener et al., 2015) and mice
328 (Takahashi et al., 2005), while *SIM1* is associated with food intake regulation and obesity (Holder
329 et al., 2004; Yang et al., 2006), therefore both possibly affecting body mass in shrews. Further of
330 note, a hypomethylated CpG in island shrews was near the pleckstrin homology domain-
331 interacting protein gene (*PHIP*), a probable regulator of insulin-like growth factor signaling
332 pathways (Farhang-Fallah et al., 2002), which reinforces the idea that insulin growth factors are
333 involved in mammalian life-history variation (Swanson & Dantzer, 2014). No clear pattern of
334 methylation direction was detected, suggesting that transcriptional regulation in both directions is
335 important for island divergence.

336 Masked shrews do not follow the classic island rule (i.e., small-bodied mammals increase
337 in size on islands) since some insular populations appear to have decreased body mass compared
338 to their mainland counterparts (e.g., Folinsbee, 1971). BPI masked shrews occur in high densities
339 (Downie, 1986; Stewart et al., 1989; Telfer, 1984), which should lead to small animals having
340 larger body size to better compete for resources (Juette et al., 2020). However, the discrepancy
341 with this expected phenotype for island shrews might be due to their diet. Previous studies have
342 shown that food scarcity contributes to the selection of smaller body size in Palearctic shrews,
343 which might also be the case for Nearctic populations (Ochocińska & Taylor, 2003; Yom-Tov &

344 Yom-Tov, 2005). Churchfield (2002) found that in locations where higher biomass resources are
345 scarce, shrews tend be smaller in size and survive by consuming less nutritional but more abundant
346 sources of food. This might also be the case for BPI shrews feeding on sand fleas. Supporting this
347 idea, top EWAS genes involved in energy homeostasis and metabolism were differentially
348 methylated between mainland-island populations (Table 3). For example, *ATP5F1A* catalyzes the
349 synthesis of ATP, the main molecule used to store and transfer energy in cells (Schapira, 2006).
350 Similarly, the zinc finger and BTB domain–containing 7c (*ZBTB7C)* gene was also differentially
351 methylated in island shrews. *ZBTB7C* is an important metabolic regulating gene for blood-glucose
352 homeostasis during fasting (Choi et al., 2019).

353 BPI shrews also showed differentially methylated sites associated to various processes
354 related to the digestive system, including peptidase activity. This is of significance as previous
355 studies noted that masked shrews on BPI have developed specialized littoral feeding habits
356 (MacPherson & Stewart, 2003; Stewart et al., 1989). Allozyme studies showed that BPI shrews
357 possess a unique polymorphism for the digestive enzyme Peptidase A, which potentially allows
358 shrews to easily digest the sand fleas' exoskeleton (McAlpine, 2009). Digestive system related
359 pathways being in the top enrichment category indicate that these dietary habits seem to be one of
360 the most significant molecular differences between this insular population and others and support
361 earlier allozyme work (MacPherson & Stewart, 2003; McAlpine, 2009). These findings
362 demonstrate that DNA methylation is one of the underlying mechanisms associated with dietary
363 divergence between Nova Scotia island and mainland masked shrew populations.

364

365

366

367 **Epigenetic age**

368 DNA methylation and chronological age can be used to build epigenetic clocks to identify genes
369 associated with aging and predict how methylation patterns change throughout an individual's
370 lifetime (Larison et al., 2021; Lu et al., 2021; Prado et al., 2021; Wilkinson et al., 2021). Epigenetic
371 clocks have been constructed for a wide range of species, showing consistent trends with CpGs
372 associated to developmental genes and pathways (Lu et al., 2021; Pinho et al., 2021; Raj et al.,
373 2021; Schachtschneider et al., 2021). Second generation clocks, such as the DNAm GrimAge,
374 account for variables such as chronological age, health factors and mortality, to predict lifespan
375 and healthspan (Bell et al., 2019; Lu et al., 2019). In humans, DNAm GrimAge has been studied
376 in relation to various comorbidities and social factors (Lu et al., 2019; McCrory et al., 2021).
377 Inbreeding has been associated with decreasing longevity and an increase in health concerns in
378 various species (Keller & Waller, 2002; Skotarczak et al., 2020; Yordy et al., 2020) and recently
379 was linked to accelerated DNAm aging in zebras (*Equus quagga*) (Larison et al., 2021). We used
380 these patterns to explore accelerated aging as a component of island-mainland divergence.

381 Masked shrews tend to live on average 14 months; accurately aging small mammals such
382 as shrews can be difficult since they are such small creatures and current methods rely on
383 somewhat subjective classification based on teeth wear, body length measurements and weight
384 (Pruitt, 1954; Rudd, 1955). Our epigenetic clock validated the current aging techniques used in the
385 field, and overall, the clock was highly predictive (R = 0.96; MAE = 0.09) (Figure 1). Further,
386 when we examined the clock model residuals, island shrews appeared to age slightly faster than
387 mainland shrews. Parasites can affect hosts' life-history traits through the energetic investment of
388 maintaining an immune system response (Cooper et al., 2012; Cowan et al., 2009; Morand &
389 Harvey, 2000), possibly resulting in faster biological aging. Group size has been shown to be

correlated with prevalence and intensity of parasitism (Coté & Poulin, 1995). The population density of shrews on BPI is extremely high, at least in some years (Downie, 1986; Stewart et al., 1989; Telfer, 1984) possibly resulting in an increased incidence of various parasites and pathogens. Overall, this study reports phenotypic trends that counter the prevailing island rule, and more broadly support the role of epigenetics in shaping phenotypic divergence. Future research should investigate epigenetic aging in insular populations, especially when inbreeding (Larison et al., 2021) or phenotypic divergence (i.e., this study) is present.

Acknowledgments

This work was supported by CanSeq150 (CGEn) (ABAS, DTS and MLC); Ontario Graduate Scholarship (MLC), Natural Sciences and Engineering Research Council of Canada (NSERC) Alexander Graham Bell Canada Graduate Scholarship-Master's (MLC) and NSERC Discovery grants (ABAS and DTS); Compute Canada Resources for Research Groups (ABAS); Canadian Foundation for Innovation: John R. Evans Leaders Fund (ABAS); Ontario Early Researcher Awards (ABAS). SH was supported by the Paul G. Allen Frontiers Group.

References

Adler, G. H., & Levins, R. (1994). The island syndrome in rodent populations. *The Quaterly Review of Biology*, *69*(4), 18–19.

al Aboud, N., Tupper, C., & Jialal, I. (2021). *Genetics, Epigenetic Mechanism*. StatPearls Publishing.

Altschup, S. F., Gish, W., Miller, W., Myers, E. W., & Lipman, D. J. (1990). Basic Local Alignment Search Tool. In *J. Mol. Biol* (Vol. 215).

Anastasiadi, D., Venney, C. J., Bernatchez, L., & Wellenreuther, M. (2021). Epigenetic inheritance and reproductive mode in plants and animals. *Trends in Ecology and Evolution*, *36*(12), 1124–1140. https://doi.org/10.1016/j.tree.2021.08.006

Anderson, S. J., Côté, S. D., Richard, J. H., & Shafer, A. B. A. (2022). Genomic architecture of phenotypic extremes in a wild cervid. *BMC Genomics*, *23*(1). https://doi.org/10.1186/s12864-022-08333-x

Arneson, A., Haghani, A., Thompson, M. J., Pellegrini, M., Kwon, S. bin, Vu, H., Maciejewski, E., Yao, M., Li, C. Z., Lu, A. T., Morselli, M., Rubbi, L., Barnes, B., Hansen, K. D., Zhou, W., Breeze, C. E., Ernst, J., & Horvath, S. (2022). A mammalian methylation array for profiling methylation levels at conserved sequences. *Nature Communications*, *13*(1), 783. https://doi.org/10.1038/s41467-022-28355-z

Baeckens, S., & van Damme, R. (2020). The island syndrome. *Current Biology*, *30*(8), R338–R339. https://doi.org/10.1016/j.cub.2020.03.029

Bairoch, A., & Apweiler, R. (1998). The SWISS-PROT protein sequence data bank and its supplement TrEMBL in 1998. In *Nucleic Acids Research* (Vol. 26, Issue 1). http://www.expasy.ch/

Bell, C. G., Lowe, R., Adams, P. D., Baccarelli, A. A., Beck, S., Bell, J. T., Christensen, B. C., Gladyshev, V. N., Heijmans, B. T., Horvath, S., Ideker, T., Issa, J. P. J., Kelsey, K. T., Marioni, R. E., Reik, W., Relton, C. L., Schalkwyk, L. C., Teschendorff, A. E., Wagner, W., … Rakyan, V. K. (2019). DNA methylation aging clocks: Challenges and recommendations. *Genome Biology*, *20*(1), 1–24. https://doi.org/10.1186/s13059-019-1824-y

Bellocq, M. I., Bendell, J. F., Innes, D. G. L., & Innes', D. G. L. (1994). Diet of Sorex cinereus, the Masked Shrew, in Relation to the Abundance of Lepidoptera Larvae in Northern Ontario. *Source: The American Midland Naturalist*, *132*(1), 68–73.

Benítez-López, A., Santini, L., Gallego-Zamorano, J., Milá, B., Walkden, P., Huijbregts, M. A. J., & Tobias, J. A. (2021). The island rule explains consistent patterns of body size evolution in terrestrial vertebrates. *Nature Ecology and Evolution*, *5*(6), 768–786. https://doi.org/10.1038/s41559-021-01426-y

Bushnell, B. (n.d.). *BBTools*. https://jgi.doe.gov/data-and-tools/bbtools/

Cao, J., Wei, C., Liu, D., Wang, H., Wu, M., Xie, Z., Capellini, T. D., Zhang, L., Zhao, F., Li, L., Zhong, T., Wang, L., Lu, J., Liu, R., Zhang, S., Du, Y., Zhang, H., & Du, L. (2015). DNA methylation Landscape of body size variation in sheep. *Scientific Reports*, *5*. https://doi.org/10.1038/srep13950

Catania, K. C., Hare, J. F., & Campbell, K. L. (2008). Water shrews detect movement, shape, and smell to find prey underwater. In *PNAS* (Vol. 105, Issue 2).

Cervantes, F. A., Arcangeli, J., & Alonso Morales, R. A. (2013). The SRY gene of the y chromosome successfully identifies gender of endemic Mexican shrews (Mammalia: Soricomorpha). *Mammalia*, *77*(3), 335–339. https://doi.org/10.1515/mammalia-2011-0123

Chai, S., Tian, R., Rong, X., Li, G., Chen, B., Ren, W., Xu, S., & Yang, G. (2020). Evidence of echolocation in the common shrew from molecular convergence with other echolocating mammals. *Zoological Studies*, *59*, 1–11. https://doi.org/10.6620/ZS.2020.59-4

Chakraborty, M., Baldwin-Brown, J. G., Long, A. D., & Emerson, J. J. (2016). Contiguous and accurate de novo assembly of metazoan genomes with modest long read coverage. *Nucleic Acids Research*, *44*(19), 1–12. https://doi.org/10.1093/nar/gkw654

Chapman, J. A., Ho, I., Sunkara, S., Luo, S., Schroth, G. P., & Rokhsar, D. S. (2011). Meraculous: De novo genome assembly with short paired-end reads. *PLoS ONE*, *6*(8). https://doi.org/10.1371/journal.pone.0023501

Chen, Y., Hu, S., Liu, M., Zhao, B., Yang, N., Li, J., Chen, Q., Zhou, J., Bao, G., & Wu, X. (2021). Analysis of Genome DNA Methylation at Inherited Coat Color Dilutions of Rex Rabbits. *Frontiers in Genetics*, *11*(January), 1–9. https://doi.org/10.3389/fgene.2020.603528

Chikhi, R., & Medvedev, P. (2014). Informed and automated k-mer size selection for genome assembly. *Bioinformatics*, *30*(1), 31–37. https://doi.org/10.1093/bioinformatics/btt310

Choi, W. il, Yoon, J. H., Song, J. Y., Jeon, B. N., Park, J. M., Koh, D. I., Ahn, Y. ho, Kim, K. S., Lee, I. K., & Hur, M. W. (2019). Zbtb7c is a critical gluconeogenic transcription factor that induces glucose-6-phosphatase and phosphoenylpyruvate carboxykinase 1 genes expression during mice fasting. *Biochimica et Biophysica Acta - Gene Regulatory Mechanisms*, *1862*(6), 643–656. https://doi.org/10.1016/j.bbagrm.2019.04.001

Churchfield, S. (1990). *The Natural History of Shrews*. Cornell University Press.

Churchfield, S. (2002). Why are shrews so small? The costs and benefits of small size in northern temperate Sorex species in the context of foraging habits and prey supply. *Acta Theriologica*, *47*, 169–184.

Cooper, N., Kamilar, J. M., & Nunn, C. L. (2012). Host longevity and parasite species richness in mammals. *PLoS ONE*, *7*(8). https://doi.org/10.1371/journal.pone.0042190

Coté, I. M., & Poulin, R. (1995). Parasitism and group size in social animals: a meta-analysis. In *Behavioral Ecology* (Vol. 6). http://beheco.oxfordjournals.org/

Cowan, K. M., Shutler, D., Herman, T. B., & Stewart, D. T. (2009). Splenic mass of masked shrews, sorex cinereus, in relation to body mass, sex, age, day of the year, and bladder nematode, liniscus (=capillaria) maseri, infection. *Journal of Parasitology*, *95*(1), 228–230. https://doi.org/10.1645/GE-1566.1

Downie, A. B. (1986). *Spatial distribution, movements and age structure in island and mainland populations of the masked shrew (Sorex cinereus Kerr)*.

Farhang-Fallah, J., Randhawa, V. K., Nimnual, A., Klip, A., Bar-Sagi, D., & Rozakis-Adcock, M. (2002). The Pleckstrin Homology (PH) Domain-Interacting Protein Couples the Insulin Receptor Substrate 1 PH Domain to Insulin Signaling Pathways Leading to Mitogenesis and GLUT4 Translocation. *Molecular and Cellular Biology*, *22*(20), 7325–7336. https://doi.org/10.1128/mcb.22.20.7325-7336.2002

Folinsbee, J. D. (1971). *Ecology of the masked shrew, Sorex cinereus, on the island of Newfoundland, Canada*.

Forsman, K. A., & Malmquist, M. G. (1988). Evidence for echolocation in the common shrew, Sorex araneus. *Journal of Zoology*, *216*(4), 655–662. https://doi.org/10.1111/j.1469-7998.1988.tb02463.x

Foster, B. (1964). Evolution of Mammals on Islands. *Nature*, *202*, 234–235.

Gardiner-Garden, M., & Frommer, M. (1987). CpG Islands in Vertebrate Genomes. *Journal of Molecular Biology*, *196*, 261–282. https://doi.org/10.1016/S0040-4020(02)00396-4

George, S. B. (1986). Evolution and Historical Biogeography of Soricine Shrews. *Systematic Biology*, *35*(2), 153–162.

George, S. B. (1988). Systematics, Historical Biogeography, and Evolution of the Genus Sorex. *Journal of Mammalogy*, *69*(3), 443–461.

Goltsman, M., Kruchenkova, E. P., Sergeev, S., Volodin, I., & Macdonald, D. W. (2005). “Island syndrome” in a population of Arctic foxes (Alopex lagopus) from Mednyi Island. *Journal of Zoology*, *267*(4), 405–418. https://doi.org/10.1017/S0952836905007557

Haas, B. J., Salzberg, S. L., Zhu, W., Pertea, M., Allen, J. E., Orvis, J., White, O., Buell, C. R., & Wortman, J. R. (2008). Automated eukaryotic gene structure annotation using EVidenceModeler and the Program to Assemble Spliced Alignments. *Genome Biology*, *9*(1), R7. https://doi.org/10.1186/gb-2008-9-1-r7

509 Haghani, A., Lu, A., Li, C., Robeck, T., Belov, K., Breeze, C., Brooke, R., Clarke, S., Faulkes,
510 C., Fei, Z., Ferguson, S., Finno, C., Gladyshev, V., Gorbunova, V., Goya, R., Hogan, A.,
511 Hogg, C., Hore, T., Kiaris, H., … Horvath, S. (2021). DNA Methylation Networks
512 Underlying Mammalian Traits. *BioRxiv*. https://doi.org/10.1101/2021.03.16.435708
513 Herridge, V. L., & Lister, A. M. (2012). Extreme insular dwarfism evolved in a mammoth.
514 *Proceedings of the Royal Society B: Biological Sciences*, *279*(1741), 3193–3200.
515 https://doi.org/10.1098/rspb.2012.0671
516 Hoff, K. J., Lomsadze, A., Borodovsky, M., & Stanke, M. (2019). *Whole-Genome Annotation*
517 *with BRAKER* (pp. 65–95). https://doi.org/10.1007/978-1-4939-9173-0_5
518 Holder, J. L., Zhang, L., Kublaoui, B. M., Dileone, R. J., Oz, O. K., Bair, C. H., Lee, Y.-H.,
519 Zinn, A. R., Lloyd, J., & Zinn, R. (2004). Sim1 gene dosage modulates the homeostatic
520 feeding response to increased dietary fat in mice. *Am J Physiol Endocrinol Metab*, *287*,
521 105–113. https://doi.org/10.1152/ajpendo.00446.2003.-Haploinsufficiency
522 Horvath, S. (2013). DNA methylation age of human tissues and cell types. *Genome Biology*,
523 *14*(10), 1–20.
524 Huggins, J. A., & Kennedy, M. L. (2018). Morphologic Variation in the Masked Shrew (Sorex
525 cinereus) and the Smoky Shrew (S . fumeus). *The American Midland Naturalist*, *122*(1),
526 11–25.
527 Humann, J. L., Lee, T., Ficklin, S., & Main, D. (2019). *Structural and Functional Annotation of*
528 *Eukaryotic Genomes with GenSAS. In: Kollmar M. (eds) Gene Prediction. Methods in*
529 *Molecular Biology* (Humana, Ed.; Vol. 1962). https://doi.org/10.1007/978-1-4939-9173-0
530 Illingworth, R. S., & Bird, A. P. (2009). CpG islands - "A rough guide." *FEBS Letters*, *583*(11),
531 1713–1720. https://doi.org/10.1016/j.febslet.2009.04.012
532 Ioshikhes, I. P., & Zhang, M. Q. (2000). Large-scale human promoter mapping using CpG
533 islands. *Nature Genetics*, *26*(1), 61–63. https://doi.org/10.1038/79189
534 Jasinska, A. J., Haghani, A., Zoller, J. A., Li, C. Z., Arneson, A., Ernst, J., Kavanagh, K.,
535 Jorgensen, M. J., Mattison, J. A., Wojta, K., Choi, O.-W., DeYoung, J., Li, X., Rao, A. W.,
536 Coppola, G., Freimer, N. B., Woods, R. P., & Horvath, S. (2021). Epigenetic clock and
537 methylation studies in vervet monkeys. *GeroScience*, *0123456789*.
538 https://doi.org/10.1007/s11357-021-00466-3
539 Johnson, R. C., Nelson, G. W., Troyer, J. L., Lautenberger, J. A., Kessing, B. D., Winkler, C. A.,
540 & O'Brien, S. J. (2010). Accounting for multiple comparisons in a genome-wide association
541 study (GWAS). *BMC Genomics*, *11*(1). https://doi.org/10.1186/1471-2164-11-724
542 Jones, P. A. (1999). The DNA methylation paradox. *Trends in Genetics*, *15*(1), 34–37.
543 https://doi.org/10.1016/S0168-9525(98)01636-9
544 Jones, P., Binns, D., Chang, H. Y., Fraser, M., Li, W., McAnulla, C., McWilliam, H., Maslen, J.,
545 Mitchell, A., Nuka, G., Pesseat, S., Quinn, A. F., Sangrador-Vegas, A., Scheremetjew, M.,
546 Yong, S. Y., Lopez, R., & Hunter, S. (2014). InterProScan 5: Genome-scale protein
547 function classification. *Bioinformatics*, *30*(9), 1236–1240.
548 https://doi.org/10.1093/bioinformatics/btu031
549 Juette, T., Garant, D., Jameson, J. W., & Réale, D. (2020). The island syndrome hypothesis is
550 only partially validated in two rodent species in an inland–island system. *Oikos*, *129*(11),
551 1739–1751. https://doi.org/10.1111/oik.07249
552 Karbiener, M., Glantschnig, C., Pisani, D. F., Laurencikiene, J., Dahlman, I., Herzig, S., Amri, E.
553 Z., & Scheideler, M. (2015). Mesoderm-specific transcript (MEST) is a negative regulator

of human adipocyte differentiation. *International Journal of Obesity*, *39*(12), 1733–1741. https://doi.org/10.1038/ijo.2015.121

Keller, L. F., & Waller, D. M. (2002). Inbreeding effects in wild populations. *Trends in Ecology and Evolution*, *17*(5), 230–241. https://doi.org/10.1016/S0169-5347(02)02489-8

Kim, D., Paggi, J. M., Park, C., Bennett, C., & Salzberg, S. L. (2019). Graph-based genome alignment and genotyping with HISAT2 and HISAT-genotype. *Nature Biotechnology*, *37*(8), 907–915. https://doi.org/10.1038/s41587-019-0201-4

Kita, M., Nakamura, Y., Okumura, Y., Ohdachi, S. D., Oba, Y., Yoshikuni, M., Kido, H., & Uemura, D. (2004). Blarina toxin, a mammalian lethal venom from the short-tailed shrew Blarina brevicauda: Isolation and characterization. *Proceedings of the National Academy of Sciences of the United States of America*, *101*(20), 7542–7547. https://doi.org/10.1073/pnas.0402517101

Kooke, R., Johannes, F., Wardenaar, R., Becker, F., Etcheverry, M., Colot, V., Vreugdenhil, D., & Keurentjes, J. J. B. (2015). Epigenetic basis of morphological variation and phenotypic plasticity in Arabidopsis thaliana. *Plant Cell*, *27*(2), 337–348. https://doi.org/10.1105/tpc.114.133025

Larison, B., Pinho, G. M., Haghani, A., Zoller, J. A., Li, C. Z., Finno, C. J., Farrell, C., Kaelin, C. B., Barsh, G. S., Wooding, B., Robeck, T. R., Maddox, D., Pellegrini, M., & Horvath, S. (2021). Epigenetic models developed for plains zebras predict age in domestic horses and endangered equids. *Communications Biology*, *4*(1). https://doi.org/10.1038/s42003-021-02935-z

Lázaro, J., Dechmann, D. K. N., LaPoint, S., Wikelski, M., & Hertel, M. (2017). Profound reversible seasonal changes of individual skull size in a mammal. *Current Biology*, *27*(20), R1106–R1107. https://doi.org/10.1016/j.cub.2017.08.055

Lázaro, J., Hertel, M., Muturi, M., & Dechmann, D. K. N. (2019). Seasonal reversible size changes in the braincase and mass of common shrews are flexibly modified by environmental conditions. *Scientific Reports*, *9*(1). https://doi.org/10.1038/s41598-019-38884-1

Lázaro, J., Nováková, L., Hertel, M., Taylor, J. R. E., Muturi, M., Zub, K., & Dechmann, D. K. N. (2021). Geographic patterns in seasonal changes of body mass, skull, and brain size of common shrews. In *Ecology and Evolution* (Vol. 11, Issue 6, pp. 2431–2448). John Wiley and Sons Ltd. https://doi.org/10.1002/ece3.7238

Lee, H. S., & Park, T. (2020). The influences of DNA methylation and epigenetic clocks, on metabolic disease, in middle-aged Koreans. *Clinical Epigenetics*, *12*(1). https://doi.org/10.1186/s13148-020-00936-z

Lokatis, S., & Jeschke, J. M. (2018). The island rule: An assessment of biases and research trends. *Journal of Biogeography*, *45*(2), 289–303. https://doi.org/10.1111/jbi.13160

Lomolino, M. v. (1985). Body Size of Mammals on Islands: The Island Rule Reexamined. *The American Naturalist*, *125*(2), 310–316. https://doi.org/10.1086/284343

Lomolino, M. v., van der Geer, A. A., Lyras, G. A., Palombo, M. R., Sax, D. F., & Rozzi, R. (2013). Of mice and mammoths: Generality and antiquity of the island rule. *Journal of Biogeography*, *40*(8), 1427–1439. https://doi.org/10.1111/jbi.12096

Lu, A. T., Fei, Z., Haghani, A., Robeck, T. R., Zoller, J. A., Li, C. Z., Zhang, J., Ablaeva, J., Adams, D. M., Almunia, J., Ardehali, R., Arneson, A., Baker, C. S., Belov, K., Blac, P., & Horvath, S. (2021). Universal DNA methylation age across mammalian tissues. *BioRxiv*, 1–28.

Lu, A. T., Quach, A., Wilson, J. G., Reiner, A. P., Aviv, A., Raj, K., Hou, L., Baccarelli, A. A., Li, Y., Stewart, J. D., Whitsel, E. A., Assimes, T. L., Ferrucci, L., & Horvath, S. (2019). DNA methylation GrimAge strongly predicts lifespan and healthspan. *Aging*, *11*(2), 303–327. https://doi.org/10.18632/aging.101684

MacPherson, I. S., & Stewart, D. T. (2003). Characterisation of a unique dipeptidase allele in an insular population of masked shrews, Sorex cinereus (Insectivora: Soricidae). *Biochemical Systematics and Ecology*, *31*(6), 573–580. https://doi.org/10.1016/S0305-1978(02)00218-1

Matsubara, K., Ishibashi, Y., Ohdachi, S., & Matsuda, Y. (2001). A new primer set for sex identification in the genus Sorex (Soricidae, Insectivora). *Molecular Ecology Notes*, *1*(4), 241–242.

McAlpine, C. S. (2009). *Molecular characterization of the unique Peptidase A Allele within a population of Sorex cinereus on Bon Portage Island, Nova Scotia*. https://scholar.acadiau.ca/islandora/object/theses:571

McCrory, C., Fiorito, G., Hernandez, B., Polidoro, S., O'Halloran, A. M., Hever, A., Ni Cheallaigh, C., Lu, A. T., Horvath, S., Vineis, P., & Kenny, R. A. (2021). GrimAge Outperforms Other Epigenetic Clocks in the Prediction of Age-Related Clinical Phenotypes and All-Cause Mortality. *Journals of Gerontology - Series A Biological Sciences and Medical Sciences*, *76*(5), 741–749. https://doi.org/10.1093/gerona/glaa286

McLain, A. T., & Faulk, C. (2018). The evolution of CpG density and lifespan in conserved primate and mammalian promoters. *Aging*, *10*(4), 561–572. https://doi.org/10.18632/aging.101413

McLean, C. Y., Bristor, D., Hiller, M., Clarke, S. L., Schaar, B. T., Lowe, C. B., Wenger, A. M., & Bejerano, G. (2010). GREAT improves functional interpretation of cis-regulatory regions. *Nature Biotechnology*, *28*(5), 495–501. https://doi.org/10.1038/nbt.1630

Meiri, S., Cooper, N., & Purvis, A. (2008). The island rule: Made to be broken? *Proceedings of the Royal Society B: Biological Sciences*, *275*(1631), 141–148. https://doi.org/10.1098/rspb.2007.1056

Meiri, S., Dayan, T., & Simberloff, D. (2006). The generality of the island rule reexamined. *Journal of Biogeography*, *33*(9), 1571–1577. https://doi.org/10.1111/j.1365-2699.2006.01523.x

Mendes-Soares, H., & Rychlik, L. (2009). Differences in swimming and diving abilities between two sympatric species of water shrews: Neomys anomalus and Neomys fodiens (Soricidae). *Journal of Ethology*, *27*(3), 317–325. https://doi.org/10.1007/s10164-008-0122-z

Meng, G., Li, Y., Yang, C., & Liu, S. (2019). MitoZ: A toolkit for animal mitochondrial genome assembly, annotation and visualization. *Nucleic Acids Research*, *47*(11). https://doi.org/10.1093/nar/gkz173

Meröndun, J., Murray, D. L., & Shafer, A. B. A. (2019). Genome-scale sampling suggests cryptic epigenetic structuring and insular divergence in Canada lynx. In *Molecular Ecology* (Vol. 28, Issue 13). https://doi.org/10.1111/mec.15131

Miller, J. M., Garant, D., Perrier, C., Juette, T., Jameson, J. W., Normandeau, E., Bernatchez, L., & Réale, D. (2021). Linking genetic, morphological, and behavioural divergence between inland island and mainland deer mice. *Heredity*. https://doi.org/10.1038/s41437-021-00492-z

Moore, L. D., Le, T., & Fan, G. (2013). DNA methylation and its basic function. *Neuropsychopharmacology*, *38*(1), 23–38.

Morand, S., & Harvey, P. H. (2000). Mammalian metabolism, longevity and parasite species richness. *Proceedings of the Royal Society B: Biological Sciences*, *267*(1456), 1999–2003. https://doi.org/10.1098/rspb.2000.1241

Nagorsen, D. (1996). *Opossums, Shrews and Moles of British Columbia*. UBC Press.

Nannini, D. R., Joyce, B. T., Zheng, Y., Gao, T., Liu, L., Yoon, G., Huan, T., Ma, J., Jacobs, D. R., Wilkins, J. T., Ren, J., Zhang, K., Khan, S. S., Allen, N. B., Horvath, S., Lloyd-Jones, D. M., Greenland, P., & Hou, L. (2019). Epigenetic age acceleration and metabolic syndrome in the coronary artery risk development in young adults study. *Clinical Epigenetics*, *11*(1). https://doi.org/10.1186/s13148-019-0767-1

Ning, Z., Giordano, F., & Harry, E. (n.d.). *Scaff10X*. https://github.com/wtsi-hpag/Scaff10X

Novosolov, M., Raia, P., & Meiri, S. (2013). The island syndrome in lizards. *Global Ecology and Biogeography*, *22*(2), 184–191. https://doi.org/10.1111/j.1466-8238.2012.00791.x

Ochocinska, D., & Taylor, J. R. E. (2003). Bergmann's rule in shrews: geographical variation of body size in Palearctic Sorex species. In *Biological Journal of the Linnean Society* (Vol. 78). https://academic.oup.com/biolinnean/article/78/3/365/2639823

Ochocińska, D., & Taylor, J. R. E. (2003). Bergmann's rule in shrews: Geographical variation of body size in Palearctic Sorex species. *Biological Journal of the Linnean Society*, *78*(3), 365–381. https://doi.org/10.1046/j.1095-8312.2003.00150.x

Ochocińska, D., & Taylor, J. R. E. (2005). Living at the physiological limits: Field and maximum metabolic rates of the common shrew (Sorex araneus). *Physiological and Biochemical Zoology*, *78*(5), 808–818. https://doi.org/10.1086/431190

Oulion, S., Bertrand, S., & Escriva, H. (2012). Evolution of the FGF Gene Family. *International Journal of Evolutionary Biology*, *2012*, 1–12. https://doi.org/10.1155/2012/298147

Pavlidis, P., Jensen, J. D., Stephan, W., & Stamatakis, A. (2012). A critical assessment of storytelling: Gene ontology categories and the importance of validating genomic scans. *Molecular Biology and Evolution*, *29*(10), 3237–3248. https://doi.org/10.1093/molbev/mss136

Pinho, G. M., Martin, J. G. A., Farrell, C., Haghani, A., Zoller, J. A., Zhang, J., Snir, S., Pellegrini, M., Wayne, R. K., Blumstein, D. T., & Horvath, S. (2021). Hibernation slows epigenetic aging in yellow-bellied marmots. *BioRxiv*, 2021.03.07.434299. https://www.biorxiv.org/content/10.1101/2021.03.07.434299v1%0Ahttps://www.biorxiv.org/content/10.1101/2021.03.07.434299v1.abstract

Posbergh, C. J., & Huson, H. J. (2021). All sheeps and sizes: a genetic investigation of mature body size across sheep breeds reveals a polygenic nature. *Animal Genetics*, *52*(1), 99–107. https://doi.org/10.1111/age.13016

Prado, N. A., Brown, J. L., Zoller, J. A., Haghani, A., Yao, M., Bagryanova, L. R., Campana, M. G., E. Maldonado, J., Raj, K., Schmitt, D., Robeck, T. R., & Horvath, S. (2021). Epigenetic clock and methylation studies in elephants. *Aging Cell*, *20*(7), 1–11. https://doi.org/10.1111/acel.13414

Pruitt, W. O. Jr. (1954). Aging in the Masked Shrew, Sorex cinereus cinereus Kerr. *Journal of Mammalogy*, *35*(1), 35–39.

Quadrana, L., & Colot, V. (2016). Plant Transgenerational Epigenetics. *Annual Review of Genetics*, *50*, 467–491. https://doi.org/10.1146/annurev-genet-120215-035254

R Core Team. (2021). *R: A language and environment for statistical computing*. R Foundation for Statistical Computing.

Raj, K., Szladovits, B., Haghani, A., Zoller, J. A., Li, C. Z., Black, P., Maddox, D., Robeck, T. R., & Horvath, S. (2021). Epigenetic clock and methylation studies in cats. *GeroScience*, *43*(5), 2363–2378. https://doi.org/10.1007/s11357-021-00445-8

Razin, A., & Riggs, D. (1980). DNA Methylation and Gene Function. *Science*, *210*(4470), 604–610.

Ritchie, M. E., Phipson, B., Wu, D., Hu, Y., Law, C. W., Shi, W., & Smyth, G. K. (2015). Limma powers differential expression analyses for RNA-sequencing and microarray studies. *Nucleic Acids Research*, *43*(7), e47. https://doi.org/10.1093/nar/gkv007

Rudd, R. L. (1955). Age, sex, and weight comparison in three species of shrews. *Journal of Mammalogy*, *36*(3), 323–338.

Saino, N., Ambrosini, R., Albetti, B., Caprioli, M., de Giorgio, B., Gatti, E., Liechti, F., Parolini, M., Romano, A., Romano, M., Scandolara, C., Gianfranceschi, L., Bollati, V., & Rubolini, D. (2017). Migration phenology and breeding success are predicted by methylation of a photoperiodic gene in the barn swallow. *Scientific Reports*, *7*(January), 1–10. https://doi.org/10.1038/srep45412

Schachtschneider, K. M., Schook, L. B., Meudt, J. J., Shanmuganayagam, D., Zoller, J. A., Haghani, A., Li, C. Z., Zhang, J., Yang, A., Raj, K., & Horvath, S. (2021). Epigenetic clock and DNA methylation analysis of porcine models of aging and obesity. *GeroScience*, *43*(5), 2467–2483. https://doi.org/10.1007/s11357-021-00439-6

Schaeffer, P. J., O'Mara, M. T., Breiholz, J., Keicher, L., Lázaro, J., Muturi, M., & Dechmann, D. K. N. (2020). Metabolic rate in common shrews is unaffected by temperature, leading to lower energetic costs through seasonal size reduction. *Royal Society Open Science*, *7*(4). https://doi.org/10.1098/rsos.191989

Schapira, A. H. (2006). Mitochondrial disease. *The Lancet*, *368*(9529), 70–82. https://doi.org/10.1016/S0140-6736(06)68970-8

Simão, F. A., Waterhouse, R. M., Ioannidis, P., Kriventseva, E. v., & Zdobnov, E. M. (2015). BUSCO: Assessing genome assembly and annotation completeness with single-copy orthologs. *Bioinformatics*, *31*(19), 3210–3212. https://doi.org/10.1093/bioinformatics/btv351

Skotarczak, E., Szwaczkowski, T., & Ćwiertnia, P. (2020). Effects of inbreeding, sex and geographical region on survival in an American bison (Bison bison) population under a captive breeding program. *European Zoological Journal*, *87*(1), 402–411. https://doi.org/10.1080/24750263.2020.1797194

Smit, A., & Hubley, R. (n.d.-a). *RepeatMasker Open-4.0*. Retrieved February 3, 2022, from http://www.repeatmasker.org

Smit, A., & Hubley, R. (n.d.-b). *RepeatModeler Open-1.0*. Retrieved February 3, 2022, from http://www.repeatmasker.org

Stewart, D. T., Herman, T. B., & Teferi, T. (1989). Littoral feeding in a high-density insular population of Sorex cinereus. *Canadian Journal of Zoology*, *67*(8), 2074–2077. https://doi.org/10.1139/z89-295

Sugrue, V. J., Zoller, J. A., Narayan, P., Lu, A. T., Ortega-Recalde, O. J., Grant, M. J., Bawden, C. S., Rudiger, S. R., Haghani, A., Bond, D. M., Hore, R. R., Garratt, M., Sears, K. E., Wang, N., Yang, X. W., Snell, R. G., Hore, T. A., & Horvath, S. (2021). Castration delays epigenetic aging and feminizes dna methylation at androgen-regulated loci. *ELife*, *10*, 1–20. https://doi.org/10.7554/eLife.64932

Swanson, E. M., & Dantzer, B. (2014). Insulin-like growth factor-1 is associated with life-history variation across Mammalia. *Proceedings of the Royal Society B: Biological Sciences*, *281*(1782). https://doi.org/10.1098/rspb.2013.2458

Takahashi, M., Kamei, Y., Ezaki, O., Takahashi, Y., & Kamei, O. E. (2005). Mest/Peg1 imprinted gene enlarges adipocytes and is a marker of adipocyte size. *Am J Physiol Endocrinol Metab*, *288*, 117–124. https://doi.org/10.1152/ajpendo

Taylor, J. R. E., Rychlik, L., & Churchfield, S. (2013). Winter reduction in body mass in a very small, nonhibernating mammal: Consequences for heat loss and metabolic rates. *Physiological and Biochemical Zoology*, *86*(1), 9–18. https://doi.org/10.1086/668484

Telfer, K. A. (1984). *Microhabitat associations, morphopology, and demography of shrews (Soricidae) in Nova Scotia*.

Thomson, V. A., Mitchell, K. J., Eberhard, R., Dortch, J., Austin, J. J., & Cooper, A. (2018). Genetic diversity and drivers of dwarfism in extinct island emu populations. *Biology Letters*, *14*(4). https://doi.org/10.1098/rsbl.2017.0617

Tomasi, T. E. (1979). Echolocation by the Short-Tailed Shrew Blarina brevicauda. In *Source: Journal of Mammalogy* (Vol. 60, Issue 4).

van Valen, L. (1973). Body Size and Numbers of Plants and Animals. *Evolution*, *27*(1), 27–35.

Vernaz, G., Hudson, A. G., Santos, M. E., Fischer, B., Carruthers, M., Shechonge, A. H., Gabagambi, N. P., Tyers, A. M., Ngatunga, B. P., Malinsky, M., Durbin, R., Turner, G. F., Genner, M. J., & Miska, E. A. (2021). Epigenetic Divergence during Early Stages of Speciation in an African Crater Lake Cichlid Fish. *BioRxiv*, *doi:10.1101/2021.07.30.435319*, 1–12.

Vernaz, G., Malinsky, M., Svardal, H., Du, M., Tyers, A. M., Santos, M. E., Durbin, R., Genner, M. J., Turner, G. F., & Miska, E. A. (2021). Mapping epigenetic divergence in the massive radiation of Lake Malawi cichlid fishes. *Nature Communications*, *12*(1), 1–13. https://doi.org/10.1038/s41467-021-26166-2

Vogt, G. (2017). Facilitation of environmental adaptation and evolution by epigenetic phenotype variation: Insights from clonal, invasive, polyploid, and domesticated animals. *Environmental Epigenetics*, *3*(1), 1–17. https://doi.org/10.1093/eep/dvx002

Wang, Y., Hannon, E., Grant, O. A., Gorrie-Stone, T. J., Kumari, M., Mill, J., Zhai, X., McDonald-Maier, K. D., & Schalkwyk, L. C. (2021). DNA methylation-based sex classifier to predict sex and identify sex chromosome aneuploidy. *BMC Genomics*, *22*(1), 1–11. https://doi.org/10.1186/s12864-021-07675-2

Weisenfeld, N. I., Kumar, V., Shah, P., Church, D. M., & Jaffe, D. B. (2018). Corrigendum: Direct determination of diploid genome sequences. *Genome Research*, *28*(4), 757–767. https://doi.org/10.1101/gr.235812.118

Whitaker John O. Jr., & French, T. W. (1984). Foods of six species of sympatric shrews from New Brunswick. *Canadian Journal of Zoology*, *62*(4), 622–626.

Wilkinson, G. S., Adams, D. M., Haghani, A., Lu, A. T., Zoller, J., Breeze, C. E., Arnold, B. D., Ball, H. C., Carter, G. G., Cooper, L. N., Dechmann, D. K. N., Devanna, P., Fasel, N. J., Galazyuk, A. V., Günther, L., Hurme, E., Jones, G., Knörnschild, M., Lattenkamp, E. Z., … Horvath, S. (2021). DNA methylation predicts age and provides insight into exceptional longevity of bats. *Nature Communications*, *12*(1). https://doi.org/10.1038/s41467-021-21900-2

Wood, D. E., & Salzberg, S. L. (2014). Kraken: Ultrafast metagenomic sequence classification using exact alignments. *Genome Biology*, *15*(3). https://doi.org/10.1186/gb-2014-15-3-r46

Yang, C., Gagnon, D., Vachon, P., Tremblay, A., Levy, E., Massie, B., & Michaud, J. L. (2006). Adenoviral-mediated modulation of Sim1 expression in the paraventricular nucleus affects food intake. *Journal of Neuroscience*, *26*(26), 7116–7120. https://doi.org/10.1523/JNEUROSCI.0672-06.2006

Yom-Tov, Y., & Yom-Tov, J. (2005). Global warming, Bergmann's rule and body size in the masked shrew Sorex cinereus Kerr in Alaska. *Journal of Animal Ecology*, *74*(5), 803–808. https://doi.org/10.1111/j.1365-2656.2005.00976.x

Yordy, J., Kraus, C., Hayward, J. J., White, M. E., Shannon, L. M., Creevy, K. E., Promislow, D. E. L., & Boyko, A. R. (2020). Body size, inbreeding, and lifespan in domestic dogs. *Conservation Genetics*, *21*(1), 137–148. https://doi.org/10.1007/s10592-019-01240-x

Zhou, W., Triche, T. J., Laird, P. W., & Shen, H. (2018). SeSAMe: Reducing artifactual detection of DNA methylation by Infinium BeadChips in genomic deletions. *Nucleic Acids Research*, *46*(20), 1–15. https://doi.org/10.1093/nar/gky691

Data accessibility statement

Raw sequence reads are deposited in the SRA: PRJNA826195

Genome is deposited in NCBI: Pending

Scripts and normalized β values for each probe and sample uploaded on GitLab:

https://gitlab.com/WiDGeT_TrentU/graduate_theses/-/tree/master/Cossette.

Benefit-sharing statement

Benefits Generated: Benefits from this research accrue from the sharing of our data and results on public databases as described above.

Author contribution:

Marie-Laurence Cossette: Methodology, Software, Formal analysis, Investigation, Data curation, Writing – original draft preparation, Visualization, Project administration, Funding acquisition. **Don T. Stewart:** Conceptualization, Methodology, Resources, Writing – review and editing, Supervision, Funding acquisition. **Amin Haghani:** Writing – review and editing,

Software, Data curation. **Joseph Zoller:** Writing – review and editing, Software, Data curation. **Aaron B.A. Shafer:** Conceptualization, Methodology, Validation, Investigation, Resources, Writing – original draft preparation, Supervision, Project administration, Funding acquisition. **Steve Horvath:** Conceptualization, Methodology, Software, Validation, Resources, Data curation, Writing – review and editing, Supervision, Project administration, Funding acquisition.

Tables and figures

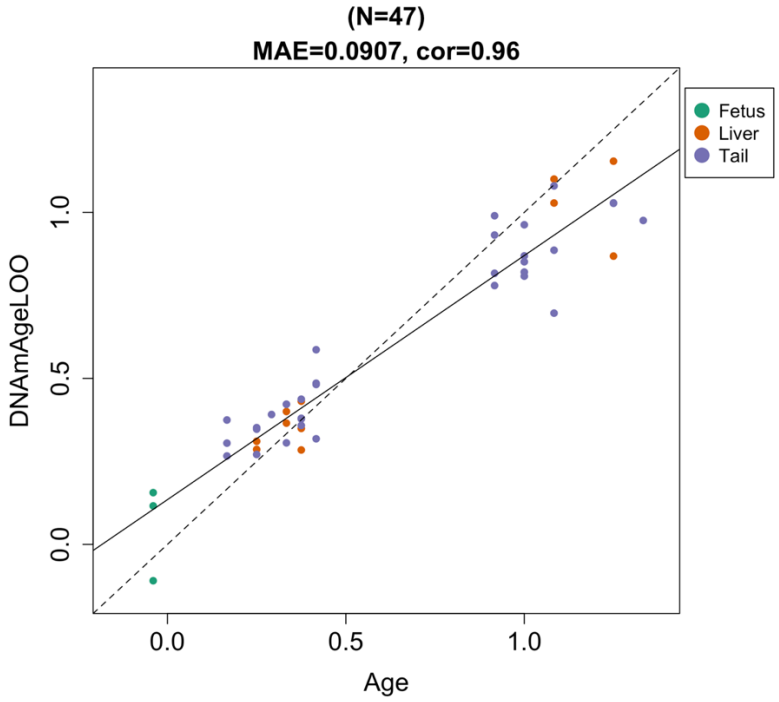

Figure 1. Cross-validation study of pan-tissue epigenetic clock for masked shrews. Leave-one-sample-out (LOO) estimate (y-axis, in units of years) versus chronological age (x-axis, in unit of years). The linear regression of epigenetic age is indicated by a solid line while the diagonal line (y = x) is depicted by a dashed line. "MAE" represents the mean absolute error and "cor" represents the correlation coefficient

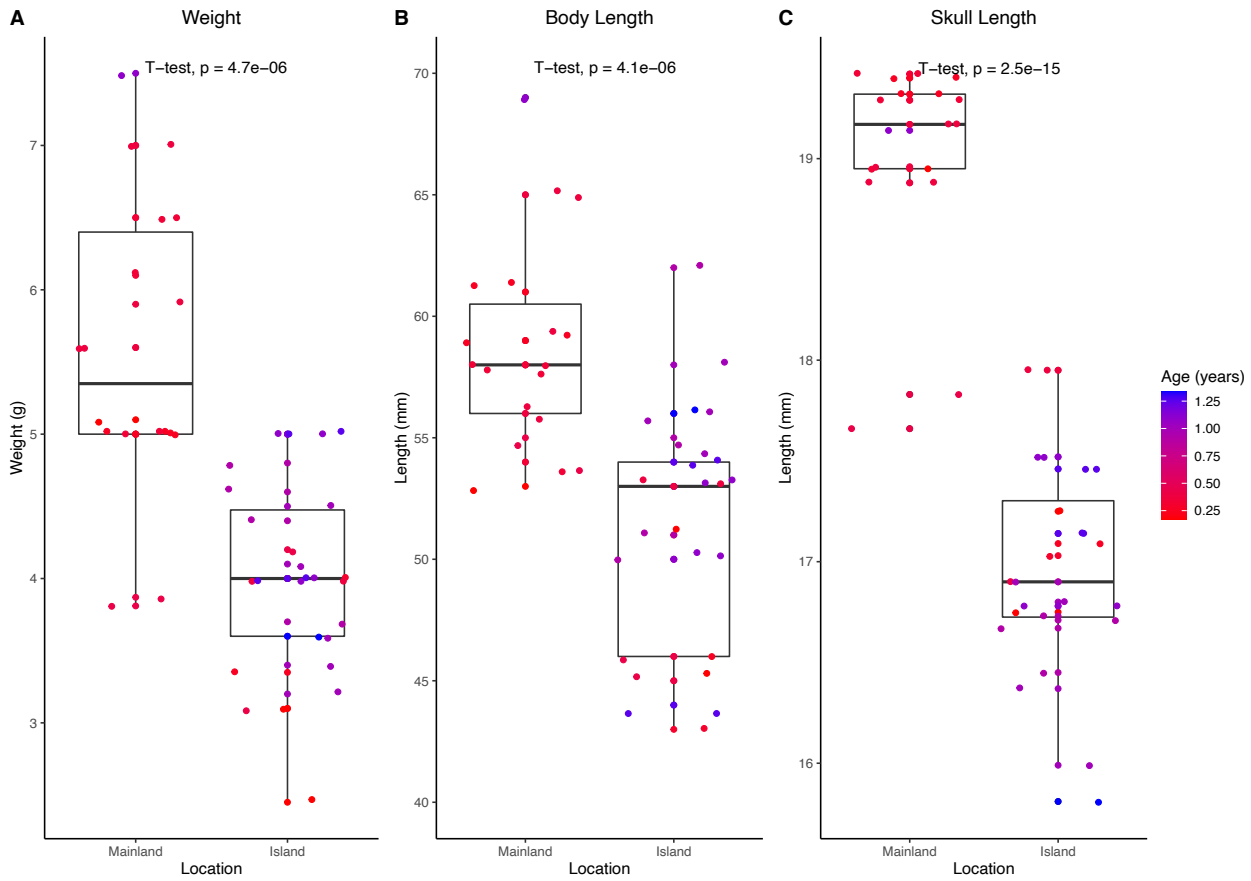

Figure 2. Boxplot of **A** weight (g), **B** body length (mm) and **C** skull length (mm) between mainland and island masked shrew populations.

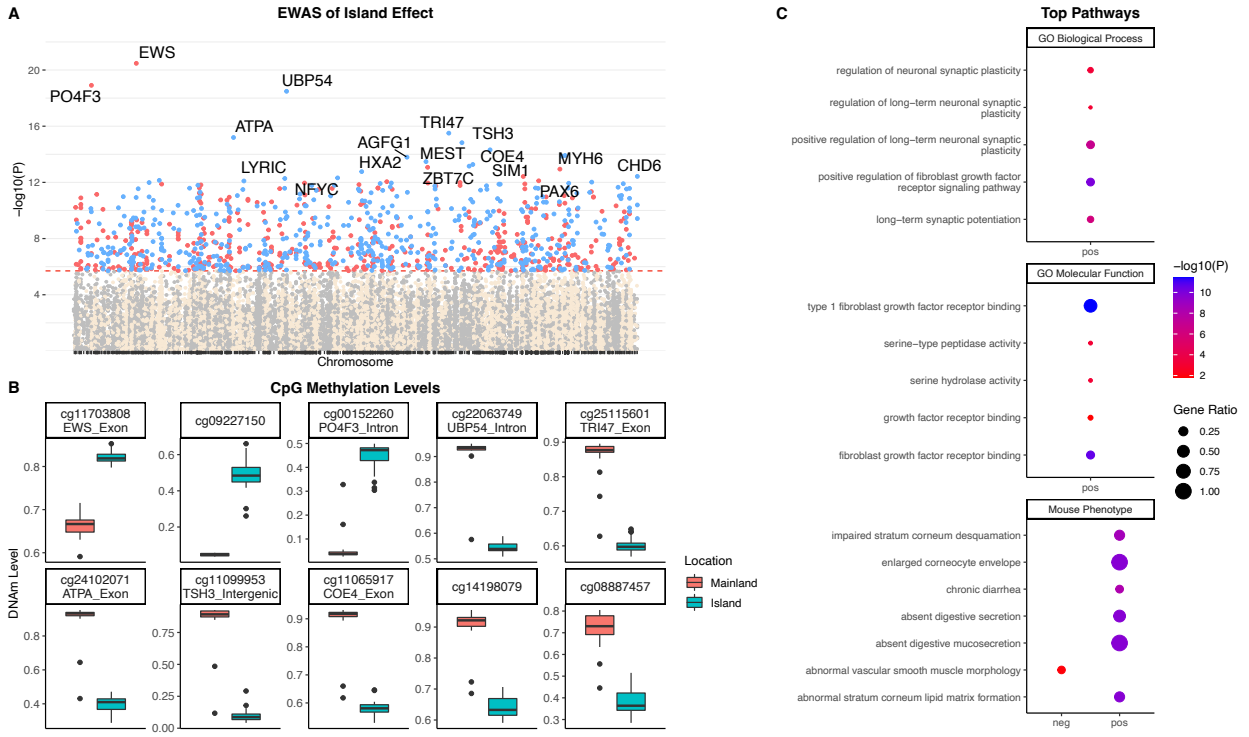

Figure 3. Epigenome-wide association (EWAS) of the multivariate regression model (location, age, sex and tissue) for masked shrew. **A** Manhattan plots of the EWAS for location (island vs mainland). The coordinates are estimated based on the alignment of Mammalian array probes to our masked shrew genome assembly. The direction of associations with < 2e-6 (red dotted line) is highlighted by red (hypermethylated) and blue (hypomethylated) colors. Top 15 CpGs are indicated by their neighboring genes. **B** DNAm levels of island samples versus mainland for the top 10 significant CpGs associated to location. **C** Enrichment analysis of the top CpGs with positive (hypermethylated) and negative (hypomethylated) correlations to island populations. The gene-level enrichment analysis was carried out using the GREAT software. Background probes were limited to 14290 probes that had shrew gene annotations. The top ontologies with most significance pathways for island samples were selected based on Bonferroni corrected p-values.

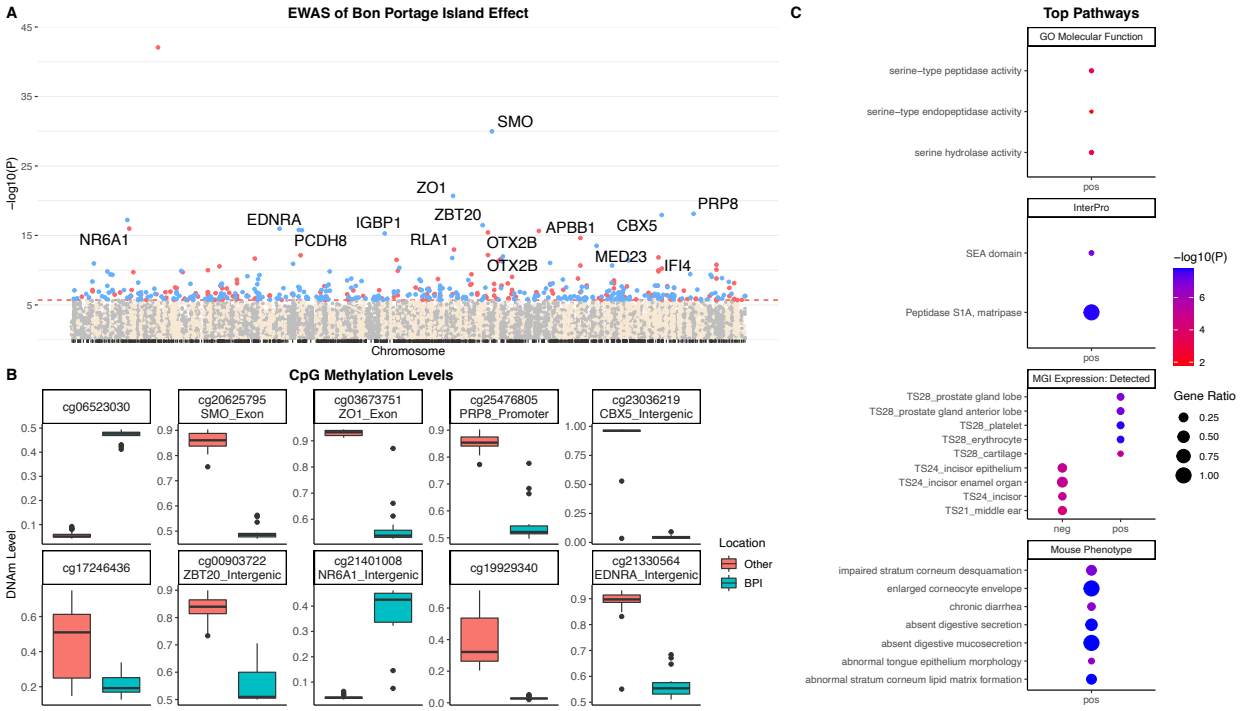

Figure 4. Epigenome-wide association (EWAS) of the multivariate regression model (location, age, sex and tissue) for masked shrew. **A** Manhattan plots of the EWAS for location (Bon Portage Island (BPI) vs others). The coordinates are estimated based on the alignment of Mammalian array probes to our masked shrew genome assembly. The direction of associations with < 2e-6 (red dotted line) is highlighted by red (hypermethylated) and blue (hypomethylated) colors. Top 15 CpGs are indicated by their neighboring genes. **B** DNAm levels of BPI samples versus others for the top 10 significant CpGs associated to location. **C** Enrichment analysis of the top CpGs with positive (hypermethylated) and negative (hypomethylated) correlations to BPI. The gene-level enrichment analysis was carried out using the GREAT software. Background probes were limited to 14290 probes that had shrew gene annotations. The top 4 ontologies with most significance pathways for BPI were selected based on Bonferroni corrected p-values.

Table 1. Trapping location of samples, N = total number of samples, number of females, minimum and maximum age. Age is represented as the estimated age in months divided by 12. Note, age of 0.00 represents fetus.

Location	Island	N	No. of females	Age (min/max)
Bon Portage Island, NS	Yes	16	6	0.167/1.33
Long Island, NS	Yes	9	4	0.00/1.25
Sandy Cove, NS	No	4	3	0.250/0.375
North Mountain, NS	No	2	1	0.417/0.417
Peterborough County, ON	No	6	1	0.167/1.08

863 **Table 2.** Summary statistics for the linear regression models for weight, body length and skull length of mainland vs
864 island masked shrews. Sex values are relative to females and location relative to mainland populations. The β-
865 coefficient (estimate), 95% confidence interval (CI), p-value and adjusted R^2 are provided.
866

	Estimate	95% CI	P value	Adj. R^2
Model 1: Weight ~ Age + Sex + Location				0.55
Age	1.20	0.39 to 2.01	**0.005**	
Sex	– 0.09	– 0.60 to 0.43	0.738	
Location	– 2.14	– 2.74 to – 1.53	**<0.001**	
Model 2: Body length ~ Age + Sex + Location				0.47
Age	6.15	1.60 to 10.69	**0.009**	
Sex	– 0.04	– 2.94 to 2.86	0.980	
Location	– 10.35	– 13.75 to – 6.94	**<0.001**	
Model 3: Skull length ~ Age + Sex + Location				0.81
Age	– 0.24	– 0.78. to 0.29	0.367	
Sex	– 0.25	– 0.59 to 0.09	0.146	
Location	– 1.93	– 2.33 to – 1.52	**<0.001**	

867
868
869 **Table 3.** Top 5 genes near outlier CpGs for island vs mainland EWAS and BPI vs all other populations. Functions
870 of each gene are abbreviated from Uniprot.
871

Gene name	CpG	Direction	Location (p)	Putative Function
Island-mainland				
EWS exon	cg11703808	pos	3.35e-21	Transcriptional repressor and might play a role in the tumorigenic process.
PO4F3 intron	cg00152260	pos	1.23e-19	Transcriptional activator. Involved in the auditory system development.
UBP54 intron	cg22063749	neg	3.27e-19	Has no peptidase activity.
TRI47 exon	cg25115601	neg	3.12e-16	Mediates the ubiquitination and proteasomal degradation of CYLD.
ATPA exon	cg24102071	neg	6.37e-16	Produces ATP from ADP
BPI				
SMO exon	cg20625795	neg	1.03e-30	Associates with the patched protein (PTCH) to transduce the hedgehog's proteins signal.
ZO1 exon	cg03673751	neg	2.00e-21	Related to movement of substances through the paracellular space. Plays a role in the regulation of cell migration.
PRP8 promoter	cg25476805	neg	7.60e-19	Plays role in pre-mRNA splicing.
CBX5 intergenic	cg23036219	neg	1.12e-18	Associated with epigenetic repression. Involved in the formation of functional kinetochore.
ZBT20 intergenic	cg00903722	neg	3.32e-17	Transcription factor that may be involved in hematopoiesis, oncogenesis, and immune responses. Plays a role in postnatal myogenesis.

872